Supporting Information for

Glutamic Acid 181 is Negatively Charged in the

Bathorhodopsin Photointermediate of Visual Rhodopsin

Megan N. Sandberg[†], Tabitha L. Amora[†], Lavoisier S. Ramos[†],

Min-Hsuan Chen[‡,||], Barry E. Knox[‡,||,], Robert R. Birge[†,*]*

[†]Department of Chemistry, University of Connecticut
[‡]Department of Biochemistry and Molecular Biology,
State University of New York Upstate Medical University
[||]Department of Ophthalmology, SUNY UMU

*Address correspondence to either: Robert R. Birge, Phone: (860) 486-6720. Fax: (860) 486-2981. E-mail: rbirge@uconn.edu or Barry E. Knox, Phone: (315) 464-8719. Fax (315) 464-8750. E-mail: knoxb@upstate.edu

Table of Contents

Figures	
S1	*Electrostatic map of bathorhodopsin with Glu-122(–) and His-211(+)*
S2	*Level ordering of the low-lying excited singlet states of bathorhodopsin based on MNDO-PSDCI molecular orbital theory*

Tables	
S1	*Protonation state assignments of Glu181 in the dark state of rhodopsin*
S2	*SAC-CI Level Three 160 x 160 results for the rhodopsin binding site*
S3	*SAC-CI Level Three 160 x 160 results for the bathorhodopsin binding site*
S4	*SAC-CI Level Three 190 x 190 results for the bathorhodopsin binding site*
S5	*SAC-CI results for bathorhodopsin assuming Glu-122(–) and His-211(+)*
S6	*Key spectroscopic observations and the implication in terms of Glu-181*

I.   Literature protonation state assignments of Glu-181

The protonation state of Glu-181 has been the subject of over seventeen experimental and theoretical studies.[1-17]   The key conclusions of these investigations are summarized in Table S1.   An excellent overview of the theoretical work on this topic can be found in Ref. 17.

Table S1. Protonation state assignments for Glu-181 in the dark state of rhodopsin.

Protonation state of E181	Method of assignment	Reference(s)
Neutral	Pre-resonance Raman spectroscopy	1
Neutral	Two-Photon Spectroscopy	2
Neutral	Low-temperature resonance Raman spectroscopy	3
Neutral	CASSCF/CASPT2 calculations	4
Charged	NMR spectroscopy	5, 6, 7,8
Charged	FT-IR spectroscopy	9, 10
Charged	Explicit solvent MD simulations	11
Charged	Time-resolved UV-Vis spectroscopy	12
Charged	MD simulations with experimental ^{2}H NMR data	13
Charged	QM/MM simulations	14
Charged	CASSCF/CASPT2 calculations	15
Inconclusive	Microsecond-scale MD simulations	16
Inconclusive	Three-layer ONIOM studies	17

II.   Materials and experimental methods

II.a. Visual pigment expression and purification

The pigments were constructed and isolated as previously reported.[18] The E181Q mutant was expressed in COS1 cells and purified by immunoaffinity chromatography techniques. The pigments were eluted in 1× buffer Y1 [50 mM HEPES, 140 mM NaCl, 3 mM $MgCl_2$, pH 6.6] with 20 % glycerol and 0.1 % DM (*N*-dodecyl-β-D-maltoside).

II.b. Cryogenic Electronic Spectroscopy

The spectra of native and E181Q bathorhodopsin were measured using our standard methods[19-22], with additional care taken to accurately assign the photoconversion percentages. Samples were prepared in 67 % glycerol, 0.05 % N-dodecyl β-D-maltoside, and 1X buffer Y1 (see above). Experiments were performed at 10 K in a closed-cycle helium-refrigerated cryostat (APD, Inc.) inserted into the optical chamber of a Cary 50 UV-vis spectrophotometer. The 10 K temperature was chosen to prevent any formation of intermediates other than bathorhodopsin. In the case of E181Q, which has a batho photoproduct that is much less stable than in the native protein, a temperature below 20 K is required. To generate the photostationary states, samples were illuminated with a Photomax system equipped with a 200 W arc lamp and a monochromator (Oriel, Stratford, CT) tuned 20 nm to the blue of the absorption maximum of the resting (dark) state. The samples were illuminated until no further spectral changes could be observed.

Two methods were used to determine the composition of the photostationary state. The first method involved warming up the sample to ambient temperature to allow the formation of meta II, which has an absorption maximum for both rhodopsin and

E181Q rhodopsin at 380 nm. The resulting spectrum contains a mixture of dark state and meta II, separated in wavelength to a sufficient extent to permit reliable spectral deconvolution.   The integral of the λ_{max} band, when compared to that observed for the pure dark state at the same temperature, permits accurate assignment of the amount of rhodopsin converted. For comparison, retinal oximes were extracted and analyzed using HPLC following the methods and procedures reported previously.[19] These two methods agreed to within 2 % and the results were averaged to obtain the fraction of species converted to the batho intermediate.   Three such experiments were carried out and the batho spectra averaged (Figure 2).   Worst-case errors in oscillator strength shifts and absorption maxima were assigned based on both the spectral and HPLC measurements.

III. Computational Methods and Additional Discussion

All molecular orbital calculations other than the MNDO-PSDCI calculations were carried out using Gaussian-09.[23] The MNDO-PSDCI calculations were carried out using our own program.[20-22,24] The MNDO-PSDCI kernel (Windows XP/7, Mac OSX 10.4 or above) and a graphical-user interface (Anamol 5.4.8) are available by request from the author (rbirge@uconn.edu). Hydrogen atoms were added by using Anamol 5.4.8. Hydrogen atoms and chromophore geometries were optimized by using the B3LYP/6-31G(d) procedures[25,26] in Gaussian-09 while holding the non-chromophore heavy atoms at the crystal geometry coordinates. The glutamine residue was optimized by minimizing the two possible rotational geometries and selecting the geometry with the lower energy. The most stable glutamine configuration is shown in the insert at right. Figures 1-3, S1 and S2 were generated in mathscriptor 1.9.38 (www.mathscriptor.org).
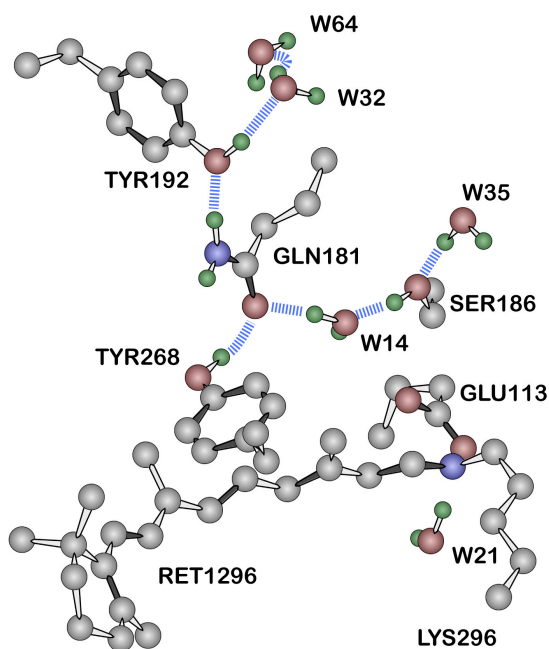
III.a.   SAC-CI calculations

The symmetry-adapted-cluster configuration-interaction method (SAC-CI)[27-30] provides a reliable theoretical procedure for investigating the spectroscopic properties of isolated and protein-bound chromophores.[27,31-34]   The strength of the method is the efficiency of the symmetry adapted cluster process which allows calculations to include a very large

configuration interaction (CI) basis set, both in terms of the number of configurations as well as the molecular size. Our calculations included the chromophore and all of the residues and water molecules shown in Figure 1. Some calculations included additional residues (see below and Figure S1). In all but one calculation, the CI basis set included the 160 highest energy filled molecular orbitals and the 160 lowest energy unfilled molecular orbitals and all possible single excitations. We refer to these as 160×160 calculations. One calculation on bathorhodopsin included a larger basis set of the 190 highest energy filled molecular orbitals and the 190 lowest energy unfilled molecular orbitals. This bathorhodopsin calculation is referred to as the 190×190 calculation and is shown in Table S2 and in Figure 3. Both the 160×160 and 190×190 bathorhodopsin calculations, when compared to the experimental data in Figure 2, strongly support a negatively charged Glu-181 residue. The analyses of the calculations on rhodopsin and bathorhodopsin are summarized in Table S6.

Unless stated otherwise, our calculations were carried out assuming Glu-122 and His-211 were both neutral, an assignment supported by FT-IR and NMR studies.[35,36] However, B3LYP/6-31G(d) calculations on the extended binding site (Figure S1) indicate that the total energy of the binding site is only ~1 kcal/mol higher if both residues are charged and form a salt bridge [E_{tot}(E122…H211) = -3567.5497211 Hartree; E_{tot}(E122$^{(-)}$…H211$^{(+)}$) = -3567.5481357 Hartree]. Thus, for comparative purposes, we also carried out calculations including the Glu-122$^{(-)}$ and His-211$^{(+)}$ salt-bridge anticipating that proximity of these charged residues to the β-ionylidene ring of the chromophore might alter our conclusions. The results are shown in Table S5. While the presence of the salt-bridge generates red shifts in the λ_{max} bands, the shifts are nearly

identical for all three systems. Thus, correct assignment of the protonation state of these residues is not critical to the assignment of the protonation state of Glu-181. The observation that the salt-bridge model has a total energy nearly identical to a neutral pair suggests that the protonation states of these residues deserve further study.

As discussed in the main portion of this paper, analysis of the bathorhodopsin calculations clearly indicate that the SAC-CI calculations are consistent with a negatively charged Glu-181 and are inconsistent with a neutral Glu-181. However, we also carried out calculations on rhodopsin, which are presented in Table S2. These calculations also support a negatively charged Glu-181, but with a level of uncertainty discussed here. A portion of the ambiguity is intrinsic to the experimental observations (Figure 2). Although the absorption maxima of rhodopsin and E181Q are separated by 9 nm at room temperature, at 10 K these spectra are only separated by 4 nm. This observation is consistent with the Glu-181 residue being near to a nodal charge-shift line (Figure 1), and generates some ambiguity when using the spectral shifts to assign protonation state. Nevertheless, the SAC-CI calculations shown in Table S2 predict that a rhodopsin binding site with a neutral Glu-181 would undergo a large blue shift in E181Q. The fact that a small red shift is observed argues against a neutral Glu-181. The observed shift is consistent with the calculations for Glu-181$^{(-)}$. Similarly, E181Q has a lower λ_{max} band oscillator strength than the native protein, which is also consistent with Glu-181$^{(-)}$ and inconsistent with a neutral Glu-181 residue (Table S2 and Figure 2). Comparison of the calculated and observed higher energy bands is difficult because the intensities appear to be temperature dependent or obscured by the broad λ_{max} band. Thus, while comparison of calculated and observed properties of the λ_{max} band favor the Glu-181$^{(-)}$ assignment,

the assignment for rhodopsin is far less compelling than the comparable assignment for bathorhodopsin. The salient conclusions of the SAC-CI calculations for both rhodopsin and bathorhodopsin are summarized in Table S6.

IIIb. MNDO-PSDCI calculations.

Although we do not suggest that semiempirical methods are optimal for the present study, we include the results of MNDO-PSDCI calculations here because these calculations provide additional perspective. Indeed, MNDO-PSDCI survey calculations were responsible for convincing us that Glu-181 was likely charged in bathorhodopsin and prompted the use of higher-level SAC-CI calculations to explore the problem in more detail. The MNDO-PSDCI methods used here are identical to those used in previous studies of the binding sites of rhodopsin and various cone pigments.[20-22,24] The present set of calculations included the chromophore and all residues within 5.6 Å of the chromophore. We assumed that Glu-122 and His-211 were both neutral. Previous studies have shown that MNDO-PSDCI methods provide good agreement with the experimental absorption spectra of rhodopsin and the cone pigments.[20-22,24] However, because the configuration interaction is limited to the chromophore, the oscillator strengths will not be calculated with accuracy and cannot be used to make assignments. This observation follows from the fact that the oscillator strength is very sensitive to configuration interaction between the chromophore and nearby aromatic residues.[37] Such interactions, while included in the SAC-CI calculations discussed above, are beyond the capability of our program when the full binding site is included. The MNDO-PSDCI results are shown in Figure S2.

The calculated transition energies predicted by the MNDO-PSDCI calculations are more consistent with a charged Glu-181 than a neutral Glu-181. These calculations predict no observable shift in absorption maximum in going from Glu-181 (neutral) to Gln-181 (E181Q). In contrast, these calculations predict a significant red shift in going from Glu-181[(-)] to Gln-181 (Figure S2), which is experimentally observed (Figure 2), although the experimental shift is smaller than calculated. The MNDO-PSDCI calculations also match the energy and intensity shifts observed in the higher energy bands better if we assume Glu-181[(-)] rather than Glu-181(neutral). Thus, these calculations add support for our conclusion that Glu-181 is negatively charged in bathorhodopsin.

Table S2. SAC-CI Level Three (160 x 160) results for dark (resting) state of rhodopsin.[a-c]

System	S#	ΔE (eV)	λ_{max} (nm)	f	%Doubles	$\Delta\mu$ (D)
E181 (0)	S1	2.8878	429.39	1.2597	9.96	20.9115
E181 (0)	S2	4.2203	293.82	0.0335	12.80	27.9702
E181 (0)	S3	4.3396	285.74	0.0066	11.27	14.2711
E181 (0)	S4	4.3576	284.56	0.2893	27.24	18.2983
E181 (0)	S5	4.3766	283.32	0.0021	10.69	14.8677
E181 (0)	S6	4.8427	256.06	0.0002	10.57	17.7251
E181 (0)	S7	5.2914	234.34	0.0233	9.46	9.6786
E181 (0)	S8	5.5824	222.13	0.1482	28.30	9.7634
E181Q	S1	3.2114	386.12	1.2654	9.71	23.2245
E181Q	S2	4.4277	280.06	0.4036	33.54	17.5604
E181Q	S3	4.6253	268.09	0.0003	10.08	15.9110
E181Q	S4	4.7072	263.43	0.0002	10.47	16.0541
E181Q	S5	4.8353	256.45	0.0483	12.20	25.4538
E181Q	S6	5.1620	240.22	0.0003	10.01	18.4528
E181Q	S7	5.2758	235.04	0.0264	9.52	10.7097
E181Q	S8	5.6075	221.13	0.1712	28.65	10.2178
E181 (-)	S1	3.2279	384.15	1.3589	9.39	31.0148
E181 (-)	S2	4.2950	288.71	0.0025	10.87	30.3509
E181 (-)	S3	4.4266	280.12	0.2821	40.22	23.1667
E181 (-)	S4	4.9699	249.50	0.2945	22.72	28.2171
E181 (-)	S5	4.9956	248.22	0.0010	10.09	19.0919
E181 (-)	S6	5.2234	237.39	0.0265	9.72	20.4790
E181 (-)	S7	5.4370	228.07	0.1408	22.37	19.1584
E181 (-)	S8	5.4557	227.29	0.0970	12.38	19.6973

[a] **System** identifies the state or substitution of the Glu-181 residue, **S#** identifies the excited singlet state, ΔE**(eV)** column gives the transition energy in eV, λ_{max} **(nm)** gives the wavelength in nm [$\lambda(nm) \approx 1240/\Delta E(eV)$], **f** is the one-photon oscillator strength, **%Doubles** is the percentage of doubly excited configurations present in the SAC-CI solution for the given excited state and $\Delta\mu$ **(D)** is the change in dipole moment associated with the excitation in Debyes. Note the E181(0) indicates Glu-181 uncharged and E181(–) indicates Glu-181 negatively charged. E181Q indicates the substitution of Glu-181 by Gln-181.

[b] Glu-122 and His-211 were not included in this calculation.

[c] The calculations included the highest energy 160 occupied molecular orbitals and the 160 lowest energy unoccupied molecular orbitals, with single and double excitation configuration interaction based on level three (maximum CISD) selection. The excited state calculations included 25,600 singles. The number of doubles varied for the three systems; 424,461 doubles for E181(0), 41,780 doubles for E181Q, and 386,363 doubles for E181(–).

Table S3. SAC-CI Level Three (160 × 160) results for the bathorhodopsin binding site.[a-d]

System	S#	ΔE (eV)	λ_{max} (nm)	f	% Doubles	Δμ (D)
E181 (0)	S1	2.2201	558.53	1.3917	37.35	22.8270
E181 (0)	S2	3.3591	369.15	0.0719	46.72	10.9292
E181 (0)	S3	4.1455	299.12	0.0009	12.14	28.3009
E181 (0)	S4	4.3065	287.94	0.0179	17.66	18.0629
E181 (0)	S5	4.4816	276.69	0.2885	18.68	17.5642
E181 (0)	S6	4.7924	258.74	0.0000	12.22	53.3397
E181 (0)	S7	5.2643	235.55	0.0279	9.60	13.3119
E181 (0)	S8	5.5483	223.49	0.0402	32.52	10.2974
E181Q	S1	2.3287	532.49	1.4519	36.13	32.0784
E181Q	S2	3.3215	373.32	0.0652	48.07	15.2872
E181Q	S3	4.0920	303.03	0.0003	14.13	15.5777
E181Q	S4	4.1621	297.93	0.0006	13.97	14.1559
E181Q	S5	4.3223	286.88	0.0430	30.14	14.3593
E181Q	S6	4.5650	271.63	0.2548	17.32	26.0128
E181Q	S7	4.7693	260.00	0.0031	13.62	15.9044
E181Q	S8	5.4939	225.70	0.0467	33.58	15.7993
E181 (-)	S1	2.5190	492.26	1.5967	20.30	38.0034
E181 (-)	S2	3.5726	347.09	0.0177	50.02	25.2856
E181 (-)	S3	3.8349	323.35	0.0003	10.99	34.4705
E181 (-)	S4	4.2788	289.80	0.0001	13.16	16.9949
E181 (-)	S5	4.6610	266.04	0.3258	14.68	32.0909
E181 (-)	S6	4.7496	261.07	0.0000	11.90	45.6349
E181 (-)	S7	5.2362	236.81	0.0329	9.43	27.0817
E181 (-)	S8	5.6232	220.52	0.0492	31.88	25.1781

[a] See (a) of Table S2

[b] The calculations included the highest energy 160 occupied molecular orbitals and the 160 lowest energy unoccupied molecular orbitals, with single and double excitation configuration interaction based on level three (maximum CISD) selection.

[c] Glu-122 and His-211 were not included in this calculation.

[d] The excited state calculations included 25,600 singles and ~477,000 doubles. The number of doubles varied slightly for the three systems.

Table S4. SAC-CI Level Three (190 x 190) results for the bathorhodopsin binding site.[a-d]

System	S#	ΔE (eV)	λ_{max} (nm)	f	% Doubles	$\Delta\mu$ (D)
E181 (0)	S1	2.2234	557.63	1.1356	58.77	25.2059
E181 (0)	S2	3.3451	370.64	0.0600	48.90	10.8822
E181 (0)	S3	3.9857	311.07	0.0010	11.45	28.7422
E181 (0)	S4	4.0389	306.98	0.0000	13.41	2238364
E181 (0)	S5	4.2698	290.37	0.1913	22.04	11.8657
E181 (0)	S6	4.6040	269.30	0.0000	12.01	53.1815
E181 (0)	S7	5.1931	238.75	0.0325	9.41	13.3464
E181 (0)	S8	5.2785	234.89	0.0001	11.04	25.5029
E181Q	S1	2.3868	519.46	1.1268	62.15	35.2717
E181Q	S2	3.3392	371.30	0.0338	54.92	14.9196
E181Q	S3	3.8976	318.10	0.0000	13.35	14.4767
E181Q	S4	3.9994	310.01	0.0002	13.12	15.5927
E181Q	S5	4.2660	290.63	0.0829	26.79	17.3824
E181Q	S6	4.4867	276.34	0.2088	21.87	23.9277
E181Q	S7	4.6888	264.43	0.0025	13.03	16.1436
E181Q	S8	5.5076	225.11	0.0438	32.97	15.5776
E181 (-)	S1	2.4522	505.60	1.3541	30.81	40.5885
E181 (-)	S2	3.5664	347.65	0.0188	51.86	25.4671
E181 (-)	S3	3.6412	340.50	0.0003	11.16	33.9500
E181 (-)	S4	4.0444	306.56	0.0001	12.97	17.0249
E181 (-)	S5	4.5446	272.82	0.0064	12.29	44.2057
E181 (-)	S6	4.5456	272.76	0.2798	16.08	28.5933
E181 (-)	S7	5.1547	240.53	0.0383	9.31	27.3145
E181 (-)	S8	5.6039	221.25	0.0542	30.77	25.2587

[a] See (a) of Table S2
[b] The calculations included the 190 highest energy occupied molecular orbitals and the 190 lowest energy unoccupied molecular orbitals, with single and double excitation configuration interaction based on level three (maximum CISD) selection.
[c] Glu-122 and His-211 were not included in this calculation.
[d] The excited state calculations included 36,100 singles. The number of doubles varied slightly for the three systems; 612,115 doubles for E181 (0), 549,403 doubles for E181Q, and 615,589 doubles for E181 (-).

Table S5. SAC-CI Level One results for the bathorhodopsin binding site including Glu-122(−) and His-211(+).[a-c]

System	S#	ΔE (eV)	λ_{max} (nm)	f	% Doubles	Δμ (D)
E181 (0)	S1	1.9874	623.93	1.5349	19.48	37.1691
E181 (0)	S2	2.8856	429.72	0.0001	12.75	12.7476
E181 (0)	S3	3.0256	409.84	0.0047	13.28	13.5210
E181 (0)	S4	3.3671	368.27	0.0090	16.07	11.9652
E181 (0)	S5	3.3963	365.10	0.0806	42.98	37.9423
E181 (0)	S6	4.5230	274.15	0.0082	33.24	43.6625
E181 (0)	S7	4.6458	266.91	0.0069	13.84	55.0162
E181 (0)	S8	5.3045	233.76	0.0254	10.09	41.0157
E181Q	S1	2.0734	598.05	1.4588	29.64	37.3715
E181Q	S2	3.0267	409.69	0.0002	12.68	23.7678
E181Q	S3	3.1737	390.71	0.0048	13.37	23.6389
E181Q	S4	3.4070	363.96	0.0748	47.80	40.6779
E181Q	S5	3.4963	354.66	0.0006	13.16	22.0333
E181Q	S6	4.3666	283.97	0.4059	19.84	39.8766
E181Q	S7	4.9423	250.90	0.0034	13.01	57.7902
E181Q	S8	5.4647	226.91	0.0429	9.66	41.4911
E181 (-)	S1	2.2376	554.16	1.5660	19.68	14.3122
E181 (-)	S2	3.5368	350.60	0.0363	37.26	8.5988
E181 (-)	S3	3.5534	348.96	0.0175	26.41	14.4322
E181 (-)	S4	3.6740	337.51	0.0019	15.41	22.7570
E181 (-)	S5	4.0078	309.40	0.0005	13.51	26.4602
E181 (-)	S6	4.1733	297.13	0.0015	12.55	34.2387
E181 (-)	S7	4.4176	280.70	0.2663	24.57	14.7990
E181 (-)	S8	5.2351	236.86	0.0316	10.06	17.6122

[a] See (a) of Table S2

[b] Glu-122(−) and His-211(+) were included in this calculation (see Fig. S1).

[c] The calculations included the highest energy 160 occupied molecular orbitals and the 160 lowest energy unoccupied molecular orbitals, with single and double excitation configuration interaction based on level one (minimum CISD) selection. The excited state calculations included 25,600 singles and ~61,000 doubles. The number of doubles varied slightly for the three systems.

Table S6. Key spectroscopic observations and the implications in terms of the protonation state of Glu-181 in the dark (resting) state and the primary stable photoproduct, Bathorhodopsin.

State[a]	Characteristic[b]	Observation[c]	Conclusion[d]
rho	Transition energy shift (λ_{max})	$\Delta E(E181Q) < \Delta E(native)$	~ E181(-)
rho	Oscillator strength shift (λ_{max})	$f(E181Q) < f(native)$	~ E181(-)
rho	Oscillator strength shifts (*higher bands*)	$f(E181Q) \sim f(native)$	*Ambiguous*
batho	Transition energy shift (λ_{max})	$\Delta E(E181Q) << \Delta E(native)$	E181(-)
batho	Oscillator strength shift (λ_{max})	$f(E181Q) < f(native)$	~E181(-)
batho	Oscillator strength shifts (*higher bands*)	$f(E181Q) > f(native)$	E181(-)

[a] The term "*rho*" refers to the resting (dark) state and "*batho*" refers to the stable, primary photoproduct, of either the native bovine rhodopsin or the E181Q mutant.

[b] The experimental data are from Figure 2.

[c] Observations involving ΔE refer to changes in the Franck-Condon maximum of the low-energy, strongly allowed λ_{max} band. Observations involving f refer to the oscillator strength of the low-energy, strongly allowed λ_{max} band or higher energy bands as assigned under "Characteristic". "Native" refers to the native (wild-type) bovine rhodopsin.

[d] Conclusion refers to the assignment based on comparison of the observed (Figure 2) and calculated (Figure 3 and Tables S2-S5) results. When preceded with "~", the assignment is tentative because the observation involved differences that are below or very close to the resolution/reliability of the SAC-CI calculations. E181(-) indicates a conclusion that Glu-181 is negatively charged in the state listed in the first column.
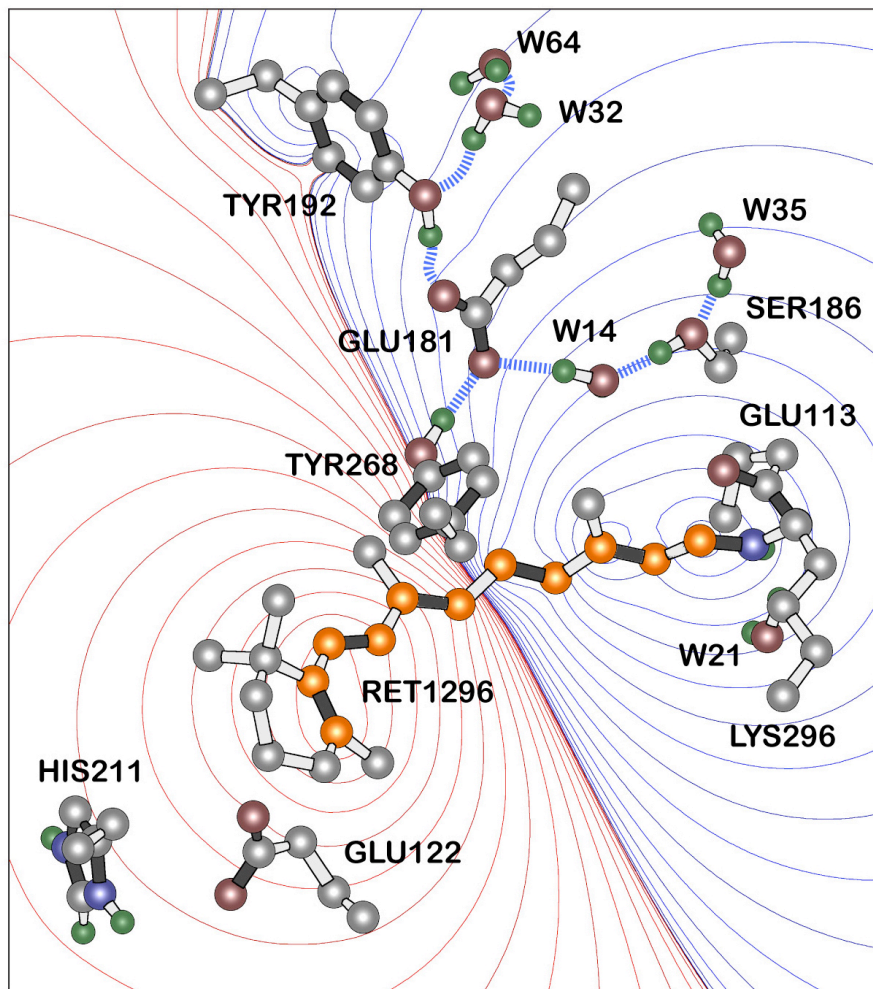
Figure S1. Charge shift upon excitation of the chromophore in bathorhodopsin into the lowest-lying strongly allowed $^1B_u^+$-like excited singlet state based on SAC-CISD calculations in which Glu-122(−) and His-211(+) are included in the calculation. Red contours indicate regions of increased positive charge, and blue contours, regions of increased negative charge. The contours are drawn at the following first-order electrostatic energies: 0 (black), ± 0.282, ± 2.26, ± 7.63, ± 18, ± 35.3, ± 61, ± 96.9, ± 144, ± 206, ± 282, ± 376, ± 488, ± 621, ± 775 kJ/mol. Key hydrogen bonds are indicated with blue dashed lines, and the polyene atoms of the retinal chromophore are shown in orange and numbered following convention. The heavy atom coordinates of the binding sites were taken from the 2G87 crystal structure of bathorhodopsin.[38] Waters are labeled using the PDB numbers minus 2000. Only polar hydrogen atoms are shown, but all hydrogen atoms were included in the calculations and were optimized along with the chromophore by using B3LYP/6-31G(d) procedures. The calculations for Glu-181(−), Glu-181(neutral) and E181Q are presented in Table S5. His-211(+) generates a small blue shift, and Glu-122(−) a larger red shift, because it is closer to the chromophore. The two residues combine to generate a small red shift.
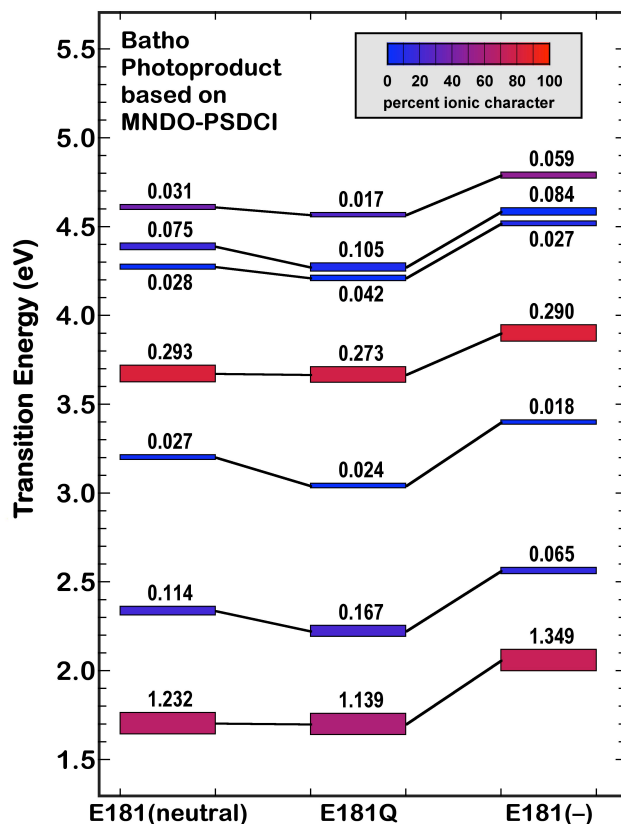
Figure S2. Level ordering of the low-lying excited singlet states of bathorhodopsin based on MNDO-PSDCI molecular orbital theory for three cases: Glu-181 neutral (left), E181Q (middle) and Glu-181 negatively charged (right). The calculations included full single and double CI within the π system of the chromophore. The covalent versus ionic character of the state is indicated by the color of the state marker and varies from blue (covalent) to red (ionic) based on the scale shown at top left. The oscillator strength of the electronic transition from the ground state is written directly above or below the state marker. The oscillator strengths are only correct to first order because the configuration interaction is limited to the chromophore.

References:

(1) Yan, E. C. Y.; Kazmi, M. A.; Ganim, Z.; Hou, J.-M.; Pan, D.; Chang, B. S. W.; Sakmar, T. P.; Mathies, R. A. *Proc. Natl. Acad. Sci. USA* **2003**, *100*, 9262-9267.

(2) Birge, R. R.; Murray, L. P.; Pierce, B. M.; Akita, H.; Balogh-Nair, V.; Findsen, L. A.; Nakanishi, K. *Proc. Natl. Acad. Sci. USA* **1985**, *82*, 4117-4121.

(3) Yan, E. C. Y.; Ganim, Z.; Kazmi, M. A.; Chang, B. S. W.; Sakmar, T. P.; Mathies, R. A. *Biochemistry* **2004**, *43*, 10867-10876.

(4) Sekharan, S.; Buss, V. *J. Am. Chem. Soc.* **2008**, *130*, 17220-17221.

(5) Mollevanger, L. C.; Kentgens, A. P.; Pardoen, J. A.; Courtin, J. M.; Veeman, W. S.; Lugtenburg, J.; de Grip, W. J. *Eur. J. Biochem.* **1987**, *163*, 9-14.

(6) Smith, S. O.; Palings, I.; Miley, M. E.; Courtin, J. M.; de Groot, H.; Lugtenburg, J.; Mathies, R. A.; Griffin, R. G. *Biochemistry* **1990**, *29*, 8158-8164.

(7) Han, M.; Smith, S. O. *Biochemistry* **1995**, *34*, 1425-1432.

(8) Honig, B.; Dinur, U.; Nakanishi, K.; Balogh-Nair, V.; Gawinowicz, M. A.; Arnaboldi, M.; Motto, M. G. *J. Am. Chem. Soc.* **1979**, *101*, 7084-7086.

(9) Nagata, T.; Terakita, A.; Kandori, H.; Shichida, Y.; Maeda, A. *Biochemistry* **1998**, *37*, 17216-17222.

(10) Lüdeke, S.; Beck, M.; Yan, E. C. Y.; Sakmar, T. P.; Siebert, F.; Vogel, R. *J. Mol. Biol.* **2005**, *353*, 345-356.

(11) Röhrig, U. F.; Guidoni, L.; Rothlisberger, U. *Biochemistry* **2002**, *41*, 10799-10809.

(12) Lewis, J. W.; Szundi, I.; Kazmi, M. A.; Sakmar, T. P.; Kliger, D. S. *Biochemistry* **2004**, *43*, 12614-12621.

(13) Martínez-Mayorga, K.; Pitman, M. C.; Grossfield, A.; Feller, S. E.; Brown, M. F. *J. Am. Chem. Soc.* **2006**, *128*, 16502-16503.

(14) Frähmcke, J. S.; Wanko, M.; Phatak, P.; Mroginski, M. A.; Elstner, M. *J. Phys. Chem. B* **2010**, *114*, 11338-11352.

(15) Tomasello, G.; Olaso-González, G.; Altoè, P.; Stenta, M.; Serrano-Andrés, L.; Merchán, M.; Orlandi, G.; Bottoni, A.; Garavelli, M. *J. Am. Chem. Soc.* **2009**, *131*, 5172-5186.

(16) Grossfield, A.; Pitman, M. C.; Feller, S. E.; Soubias, O.; Gawrisch, K. *J. Mol. Biol.* **2008**, *381*, 478-486.

(17) Hall, K. F.; Vreven, T.; Frisch, M. J.; Bearpark, M. J. *J. Mol. Biol.* **2008**, *383*, 106-121.

(18) Babu, K. R.; Dukkipati, A.; Birge, R. R.; Knox, B. E. *Biochemistry* **2001**, *40*, 13760-13766.

(19) Vought, B. W.; Dukkipati, A.; Max, M.; Knox, B. E.; Birge, R. R. *Biochemistry* **1999**, *38*, 11287-11297.

(20) Kusnetzow, A.; Dukkipati, A.; Babu, K. R.; Singh, D.; Vought, B. W.; Knox, B. E.; Birge, R. R. *Biochemistry* **2001**, *40*, 7832-7844.

(21) Ramos, L. S.; Chen, M. H.; Knox, B. E.; Birge, R. R. *Biochemistry* **2007**, *46*, 5330-5340.

(22) Kusnetzow, A. K.; Dukkipati, A.; Babu, K. R.; Ramos, L.; Knox, B. E.; Birge, R. R. *Proc. Natl. Acad. Sci. USA* **2004**, *101*, 941-6.

(23) Frisch, M. J. T., G. W.; Schlegel, H. B.; Scuseria, G. E.; Robb, M. A.; Cheeseman, J. R.; Scalmani, G.; Barone, V.; Mennucci, B.; Petersson, G. A.; Nakatsuji, H.; Caricato, M.; Li, X.; Hratchian, H. P.; Izmaylov, A. F.; Bloino, J.; Zheng, G.; Sonnenberg, J. L.; Hada, M.; Ehara, M.; Toyota, K.; Fukuda, R.; Hasegawa, J.; Ishida, M.; Nakajima, T.; Honda, Y.; Kitao, O.; Nakai, H.; Vreven, T.; Montgomery, Jr., J. A.; Peralta, J. E.; Ogliaro, F.; Bearpark, M.; Heyd, J. J.; Brothers, E.; Kudin, K. N.; Staroverov, V. N.; Kobayashi, R.; Normand, J.; Raghavachari, K.; Rendell, A.; Burant, J. C.; Iyengar, S. S.; Tomasi, J.; Cossi, M.; Rega, N.; Millam, N. J.; Klene, M.; Knox, J. E.; Cross, J. B.; Bakken, V.; Adamo, C.; Jaramillo, J.; Gomperts, R.; Stratmann, R. E.; Yazyev, O.; Austin, A. J.; Cammi, R.; Pomelli, C.; Ochterski, J. W.; Martin, R. L.; Morokuma, K.; Zakrzewski, V. G.; Voth, G. A.; Salvador, P.; Dannenberg, J. J.; Dapprich, S.; Daniels, A. D.; Farkas, Ö.; Foresman, J. B.; Ortiz, J. V.; Cioslowski, J.; Fox, D. J. Gaussian, Inc., Wallingford CT, 2009. In *Revision A.1*; Gaussian, Inc., Wallingford CT: 2009.

(24) Amora, T. L.; Ramos, L. S.; Galan, J. F.; Birge, R. R. *Biochemistry* **2008**, *47*, 4614-4620.

(25) Becke, A. D. *J. Phys. Chem.* **1993**, *98*, 5648-5652.

(26) Lee, C.; Yang, W.; Parr, R. G. *Phys. Rev. B: Condens. Matter* **1988**, *37*, 785-9.

(27) Nakajima, T.; Nakatsuji, H. *Chem. Phys.* **1999**, *242*, 177-193.

(28) Nakatsuji, H. *Chem. Phys. Lett.* **1978**, *59*, 362-4.

(29) Nakatsuji, H.; Hirao, K. *J. Chem. Phys.* **1978**, *68*, 2053-65.

(30) Nakatsuji, H. *Chem. Phys. Lett.* **1991**, *177*, 331-7.

(31) Ishida, M.; Toyota, K.; Ehara, M.; Frisch, M. J.; Nakatsuji, H. *J. Chem. Phys.* **2004**, *120*, 2593-2605.

(32) Miyahara, T.; Tokita, Y.; Nakatsuji, H. *J. Phys. Chem. B* **2001**, *105*, 7341-7352.

(33) Miyahara, T.; Nakatsuji, H.; Hasegawa, J.; Osuka, A.; Aratani, N.; Tsuda, A. *J. Chem. Phys.* **2002**, *117*, 11196-11206.

(34) Premvardhan, L.; Sandberg, D. J.; Fey, H.; Birge, R. R.; Buchel, C.; Grondelle, R. v. *J. Phys. Chem. B* **2008**, *112*, 11838-11853.

(35) Fahmy, K.; Jäger, F.; Beck, M.; Zvyaga, T. A.; Sakmar, T. P.; Siebert, F. *Proc. Natl. Acad. Sci. USA* **1993**, *90*, 10206-10210.

(36) Patel, A. B.; Crocker, E.; Reeves, P. J.; Getmanova, E. V.; Eilers, M.; Khorana, H. G.; Smith, S. O. *J. Mol. Biol.* **2005**, *347*, 803-812.

(37) Ren, L.; Martin, C. H.; Wise, K. J.; Gillespie, N. B.; Luecke, H.; Lanyi, J. K.; Spudich, J. L.; Birge, R. R. *Biochemistry* **2001**, *40*, 13906-13914.

(38) Nakamichi, H.; Okada, T. *Angew. Chem., Int. Ed.* **2006**, *45*, 4270-4273.